Solar Energy 248 (2022) 76–87

Contents lists available at ScienceDirect

Solar Energy

journal homepage: www.elsevier.com/locate/solener

The influence of icephobic nanomaterial coatings on solar cell panels at high latitudes

Mattia Manni [a,*], Maria Chiara Failla [a], Alessandro Nocente [b], Gabriele Lobaccaro [a], Bjørn Petter Jelle [a]

[a] Department of Civil and Environmental Engineering, Faculty of Engineering, Norwegian University of Science and Technology (NTNU), 7491 Trondheim, Norway
[b] SINTEF AS, 7495 Trondheim, Norway

ARTICLE INFO

Keywords:
Icephobic
Nanomaterial
Snow loss
Building-integrated photovoltaics
Solar cell

ABSTRACT

Solar energy's penetration at high latitudes has been boosted during recent years, but snow deposits during the winter still limit its exploitation. Therefore, various solutions for snow removal, such as icephobic coatings, increasing panels' tilt angle, and using wind flows, are being attempted to reduce snow and ice accumulation. The novelty of this study is that it presents insights into the snow-related issues of photovoltaic plants in Norway and proposes a preliminary approach to modelling these issues' influences at high latitudes using a co-simulation approach. The workflow is based on a combination of PVsyst and Marion's algorithm, and moves from the assessment of snow deposits on photovoltaic panels and the consequent reduction of plane of array (POA) irradiance (snow losses) to evaluating the influence of icephobic nanomaterials on snow losses. Solar analyses are performed on a photovoltaic plant located in Trondheim, Norway, and then reiterated considering the climate of the Norwegian cities of Bergen and Oslo. The snow losses between November and April, when the snow depth is greater than zero, are 32.75 kWh/m^2 in Oslo, 25.05 kWh/m^2 in Trondheim, and 5.85 kWh/m^2 in Bergen. The application of icephobic coatings currently available on the market will reduce such snow losses to 12.05 kWh/m^2 (65% efficiency) in Oslo, 10.00 kWh/m^2 (60% efficiency) in Trondheim, and 3.35 kWh/m^2 (45% efficiency) in Bergen. In conclusion, the application of icephobic coatings should be more greatly boosted in a continental climate (Oslo and Trondheim) than in an oceanic climate (Bergen) to maximize photovoltaic power output.

1. Introduction

Public interest in solar energy is rapidly increasing in Norway, as demonstrated by the increment in the installed solar power capacity from 15 MW (2015) to 225 MW (2021) over only six years (Fig. 1) (Statista, 2022), and building-integrated photovoltaics (BIPV) (Jelle, 2016; Jelle et al., 2012; Manni et al., 2020) will likely increase in popularity in the coming years. The misconception that the level of solar radiation is lower in the Nordic countries than in Continental Europe has partially contributed to this delay in the exploitation of solar energy (Formolli et al., 2021). However, recent studies regarding solar energy have demonstrated that the available solar radiation in the Nordic countries is simply differently distributed over the year if compared as compared to Continental Europe; i.e., most irradiation is available during the summer months, and only a limited amount is available during the winter. Furthermore, the average hourly direct normal irradiation on the horizontal plane can, in winter months such as February (251 Wh/m^2), reach almost the same value as in June (253 Wh/m^2) (Good et al., 2014). The sun elevation also changes significantly throughout the year; the sun height at noon in the summer is around 50°, while in the wintertime, it is below 10° (Lobaccaro et al., 2017a; Manni et al., 2018).

In this context, it has been demonstrated that installing photovoltaic (PV) systems at high latitudes has certain advantages, ranging from (i) higher efficiency due to the low temperatures to (ii) the significant amount of solar energy reflected by the snow covering the ground; (iii) the solar energy potential, especially on vertical surfaces, i.e., building facades, due to the low angle of solar rays at high latitudes; and (iv) the significant amount of annual sun hours, which is higher than in others locations in central Europe (Dubey et al., 2013; Formolli et al., 2021; Scharmer Grief, 2000). On the other hand, some barriers can be easily identified, particularly during the winter, such as the presence of snow deposits on PV panels. This snow cover can cause worsen the efficiency of grid-connected PV systems by around 3% in Continental Europe (Becker et al., 2008), but the extent to which snow influences the plane

* Corresponding author.
E-mail address: mattia.manni@ntnu.no (M. Manni).

https://doi.org/10.1016/j.solener.2022.11.005
Received 11 July 2022; Received in revised form 12 October 2022; Accepted 4 November 2022

Nomenclature

Variables

POA	Plane of array [kWh/m^2]
SL	Snow losses [kWh/m^2]
SD	Snow depth [cm]
T	Temperature [°C]
m	Empirical coefficient in Marion's algorithm [W/m^{2}K]
k	Sliding coefficient [unitless]
S	Shear force [Pa]
P	Load pressure [Pa]

Greek letters

θ	Contact angle between the liquid–vapour interface and the solid surface [0°-180°]
γ	Tension force [N/m]
β	Tilt angle of the photovoltaic panels [0°-90°]

Subscripts

L-A	Liquid-air interface
S-L	Solid-liquid interface
S-A	Solid-air interface
a	Air

Acronyms

BIPV	Building integrated photovoltaic
PV	Photovoltaic
ZEB	Zero emission building
Lab	Laboratory
MA	Marion's algorithm
VBPV	Vertically mounted bifacial photovoltaic
TMY	Typical meteorological year
NOAA	National Oceanic and Atmospheric Administration
NCDC	National Climatic Data Center
MET	Meteorological Institute
IAM	Incidence angle modifier

of array (POA) irradiance of a PV panel in Norway is has been only sparsely explored in the literature. Şevik and Aktaş examined snow-induced power losses by investigating the effects of natural and manual cleaning on the performance of PV arrays. In a three-day period, 50–75% higher energy production was achieved as compared to the other power plants with snow load. Snow removal from PV arrays both prevented PV degradation and resulted in increased power generation, while panel cleaning improved energy efficiency (Şevik and Aktaş, 2022).

The continuous monitoring of the PV systems integrated into the roof of the Zero Emission Building (ZEB) Living Laboratory (Lab) in Trondheim, Norway, shows that the optimized configuration of the PV panels (i.e., the tilt angle is designed to maximize the POA irradiance) do not prevent snow deposits, thus substantially decreasing energy production during the winter (Fig. 2). The observations from the ZEB Living Lab (Nocente et al., 2021), a pilot office building at Norwegian University of Science and Technology Gløshaugen Campus, in Trondheim, confirmed the issues of snow deposition for buildings at high latitudes (Fig. 3). Further investigations highlighted the fact that another problem that prevents the snow from sliding is the module frame: the snow cover usually sticks to the frame and slides off only partially (Fig. 2).

Because snow and ice represents a serious problem and, thus, a challenge to be solved for solar cells (Andersson et al., 2017; Borrebæk et al., 2021, 2020; Jelle et al., 2016; Midtdal and Jelle, 2013), several numerical models have been implemented to estimate and predict snow losses (SL) (Andrews et al., 2013a), which are defined as the fraction of the POA irradiance that cannot be harvested due to snow deposits, hereinafter referred to as "snow losses." The algorithm coded by (Ross, 1995) uses the surface temperature of photovoltaic solar cells as a predictor of snow coverage, i.e., ice and snow deposits if the surface temperature is below the 0 °C, while (Powers et al., 2010) found an empirical correlation between SL and both the PV tilt angle and snow depth (SD). Nonetheless, the experimental validation performed by (Andrews et al., 2013b) demonstrated that these numerical models tend to underestimate the effects of snowfalls. A turning point in modelling SL is represented by the algorithm developed by Marion et al. (Marion et al., 2013). A large dataset was used for its implementation, which included information about energy production, SDs, snow coverage, and POA irradiance for 24 combinations of PV technology, panel tilt angle, and location. In a comparative analysis of SL models performed by (Øgaard et al., 2021), Marion's algorithm (MA) yielded the best results. Therefore, MA has been chosen to be integrated into the workflow of this study (see the Methodology section for a detailed description of the algorithm).

At the same time, solutions for snow removal that do not imply additional energy consumption have been developed (Andenæs et al., 2018). In fact, manual snow removal has never been considered a valid solution because solar systems can be difficult to reach in winter and such an operation might damage the equipment (Ross, 1995). Developed techniques aim to enhance parameters of PV panels that influence snow and ice accumulation, i.e., geometrical properties, orientation, position, location, and surface physical characteristics. Increasing the tilt angle of the photovoltaic panel, as well as exploiting wind flows, may limit the adhesion of snow and ice (Ross, 1995). In that regard, vertically

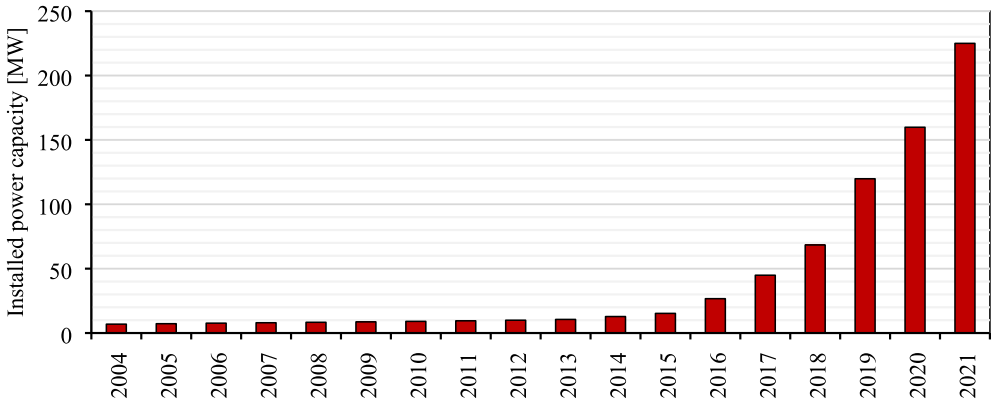

Fig. 1. Development of installed capacity for solar power in Norway (Statista, 2022).

Fig. 2. ZEB Living Lab after a snowfall in late January 2015 (left); The snow cover sticks to the frame and slides off only partially after a snowfall in late November 2015 (middle); detail of the roof geometry with the tilted and flat parts, the weather station and the three rows of modules installed and the lowest part free from the PV modules (right). Photo credit: Clara Good.

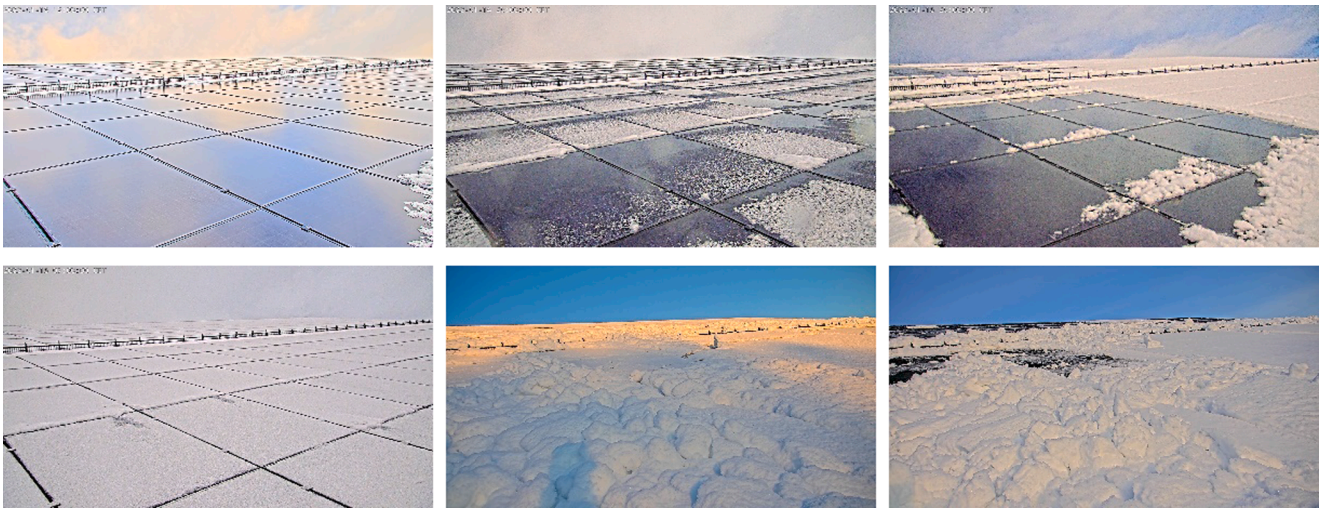

Fig. 3. From the top left corner to the bottom right corner, there is a progressive increase in the snow deposits on the PV system integrated into the rooftop of the ZEB Laboratory in Trondheim, Norway.

mounted bifacial PV (VBPV) panels (Jouttijärvi et al., 2022) or PV panels integrated into a building's façade (Tina et al., 2021) can be particularly advantageous at high latitudes due to both favorable solar geometry and conditions, i.e., low incident angles on the part of sunrays, and the presence of the snow covering the ground during some periods of the year, especially at wintertime, i.e., solar radiation reflected from the ground. Moreover, east–west oriented VBPV panels may shift energy production from noon to morning and evening, thus improving the match between solar power production and electricity load (Jouttijärvi et al., 2022). Similarly, nanoscale modifications of the PV panel surface have been implemented to create a water-repellent and self-cleaning layer. However, among the other related issues, the snow sliding off the solar cells should never constitute a danger for people walking next to the plant or an obstacle on the pathway (Jelle, 2013). This has led, for example, to the installation of anti-avalanche systems on the ZEB Laboratory (Fig. 3).

The repellent-surface strategy in the presence of snow and ice has been largely debated in the literature, leading to the development of innovative and potentially icephobic nanomaterials. Icephobic treatments have been attracting increasing interest due to their multiple applications, e.g., power lines, plane wings, and wind turbines. Regarding the energy sector, the implementation of a transparent, anti-reflective, and durable icephobic treatment for PV modules can increase energy production throughout the year, particularly during the winter season, in cold climates.

The Norwegian climate is characterized by frequent snowfalls during the winter period, which prevent the PV solar cells installed on flat and moderate tilted angles roofs from fully harvest solar irradiance, leading to reduced potential and performance in terms of energy generation. Maintaining the surfaces of the PV panels as free from snow deposits as possible should therefore be prioritized. In that regard, snow- and icephobic coatings have been demonstrated to have good potential, and they have been specifically developed for PV solar cells so as to improve their efficiency during the wintertime.

Within this framework, the novelty of the present study is in proposing a co-simulation approach to model the influence of icephobic nanomaterial coatings at high latitudes. The presented workflow couples commonly used computation and analysis tools, such as PVsyst, and advanced algorithms from the literature, such as the MA, for SL calculation to simulate the presence of snow and preliminarily estimate the POA irradiance of PV panels treated with icephobic nanomaterial coatings. Although a significant number of publications have assessed the application of snow- and icephobic coatings, the extent to which these surface treatments can influence POA irradiance in Norway remains unclear.

Thus, moving from the assessment of snow conditions in the three most populated cities of Norway (Oslo, at latitude 59.9139° N; Bergen, at latitude 60.3913° N; and Trondheim, at latitude 63.4305° N), this new study aims to numerically investigate the efficiency of PV solar cells treated with the icephobic coatings currently available on the market by comparing their performance levels against those of PV solar cells without icephobic coatings. Furthermore, an insight into the functioning of icephobic coatings and their characteristics is provided.

The study presented herein is structured as follows: the Background section (Section 2) outlines a theoretical framework for ice-formation processes, hydrophobic and superhydrophobic materials, and icephobic materials; the Materials and Methods section (Section 3) defines the research workflow, the numerical model for the estimation of SL, the

settings for the simulated materials, and the information on the selected locations; the Results and Discussion section (Section 4) provides an overview of the impacts of icephobic coatings on SL, followed by comments on the results and limitations of the study. The article concludes by considering future developments and summarizes the most important findings and the implications for future advancements in the application of icephobic nanomaterials at high latitudes (Section 5).

2. Background

2.1. Ice formation

The formation of ice and snow on a PV panel's surface may occur due to four phenomena: crystallization, moisture condensation, water desublimation, and snowfall. The crystallization process mainly consists of two phases: nucleation and crystal growth. Nucleation takes place when the liquid is exposed to a temperature below its equilibrium state and begins crystallizing. Solute molecules that are dispersed in the solvent begin gathering into clusters at nanoscale (nucleation). Then, the crystals grow until the clusters reach a critical size and become stable nuclei (crystallization). If the critical size is not achieved, the clusters dissolve. Moisture condensation is observed when the air temperature drops below the dew point and water vapor in the air becomes liquid. The condensation of water can be responsible for the formation of ice if it begins freezing. On the other hand, water desublimation can occur onto a cold surface, often by forming small ice crystals. In this case, water vapor in cold air freezes without becoming liquid water. Snow consists of flakes of crystalline ice that have formed in clouds at temperatures below 0 °C and fallen to the ground via precipitation. Snow precipitation can be observed even when air temperature values are greater than 0 °C. However, the air temperature, together with the wind velocity and characteristics of the PV panel, i.e., tilt angle and roughness, determine the snow deposited. The surface temperature of the panel also influences snow adhesion; if the surface temperature is higher than 0 °C, a thin layer of water is generated on the ice, one with hybrid properties, i.e., an intermediate between ice and water.

Once the freezing process is completed, ice adhesion plays a key role in the duration of both ice and snow obstruction. The substrate characteristics, ice particle size, and mode of fracture (i.e., the opening crack and edge sliding crack) determine ice adhesion (Fillion et al., 2014). Therefore, icephobic surfaces are designed to reduce ice adhesion and delay water freezing, mainly by affecting two parameters: nucleation temperature and nucleation delay time. To enhance these parameters, the physical properties to be implemented in icephobic coatings are mostly the same as those characterizing water-repellent surfaces. This represents an advantage because water repulsion has been more thoroughly debated by scholars than icephobicity, which property is a relatively recent and thus immature topic.

2.2. Hydrophobic and superhydrophobic coatings

The hydrophobicity level of a material is determined by the contact angle (θ) between the liquid–vapour interface and the solid surface. A surface is called hydrophilic if θ is lower than 90°; otherwise, the surface is classified as hydrophobic (90° > θ > 150°) or superhydrophobic (θ > 150°) (Fig. 4).

A given system of solid, liquid, and vapour at a given temperature and pressure has a unique equilibrium contact angle, which can be numerically estimated under specific conditions, i.e., a smooth and homogeneous solid surface. Firstly, the equilibrium of the vertical components of the interfacial tension forces is described as follows:

$$\gamma_{L-A}\cdot\cos\theta + \gamma_{S-L} = \gamma_{S-A} \quad (1)$$

where $\gamma_{L\text{-}A}$ is the liquid–air tension force, $\gamma_{S\text{-}L}$ is the solid–liquid tension force, and $\gamma_{S\text{-}A}$ is the solid-air tension force. Solving this equation for cos θ permits us to obtain Young's equation (Parvate et al., 2020) and determine whether a surface has a hydrophobic or hydrophilic nature.

If the solid-air tension force is higher than the solid–liquid tension force ($\gamma_{S\text{-}A} > \gamma_{S\text{-}L}$), the contact angle θ will be lower than 90°, and the liquid is said to "partially wet the surface." Otherwise, if the solid-air tension force is lower than the solid–liquid tension force ($\gamma_{S\text{-}A} < \gamma_{S\text{-}L}$), the contact angle θ ranges between 90° and 180°, and the liquid is said to "not wet the surface." Therefore, hydrophobicity increases when the solid-air tension force ($\gamma_{S\text{-}A}$) decreases. Hydrophobicity can be also enhanced by manipulating the topography of the surface.

For a nanorough surface, two states, i.e., the Wenzel state and the Cassie-Baxter state, are observed depending on the drop's penetration into the asperities of the surface (Fig. 5). The Wenzel state occurs when the drops' bottoms penetrate into the asperities, while air is trapped between the water and surface texture in the Cassie-Baxter state. As the surface roughness increases, it becomes unlikely for water to completely adhere to the topography of the substrate, and hydrophobicity is enhanced. Nonetheless, the system usually transitions from the Cassie-Baxter state to the Wenzel state through an irreversible process; therefore, contact time must be considered.

The coatings having a contact angle θ higher than 150° are termed superhydrophobic coatings. Such coatings have attracted great attention because they combine water-repellent properties with self-cleaning ability. In fact, a droplet rolling on a surface can drag dust away (Midtdal and Jelle, 2013).

The Cassie-Baxter state is dominant when considering super-hydrophobic coatings; therefore, highly nanorough textures are designed. Several methods have been developed to realize the hydrophobization of a surface such as covalent layer-by-layer assembly, chemical vapor deposition, the synthesis of gels and nanoparticles, and hydrothermal synthesis (Xue et al., 2010). Alongside these, approaches to producing superhydrophobic coatings exist, and these are based on the application of low-surface-energy materials onto the substrate, e.g., fluorochemicals, silicones, and nano-textured materials). However, their mechanical stability represents an issue: nanoroughness can easily be destroyed by external forces, e.g., accidental impacts or excessive wind pressure, and adhesion to the substrate is weak most of the time.

2.3. Icephobic coatings

Icephobic coatings consist of materials capable of delaying ice

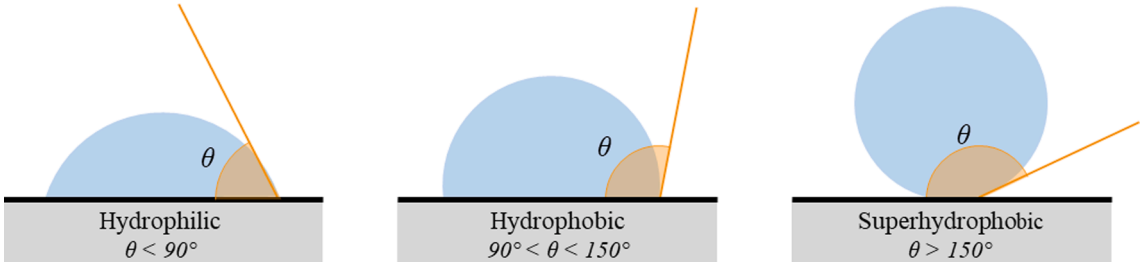

Fig. 4. Surface properties depending on the contact angle θ.

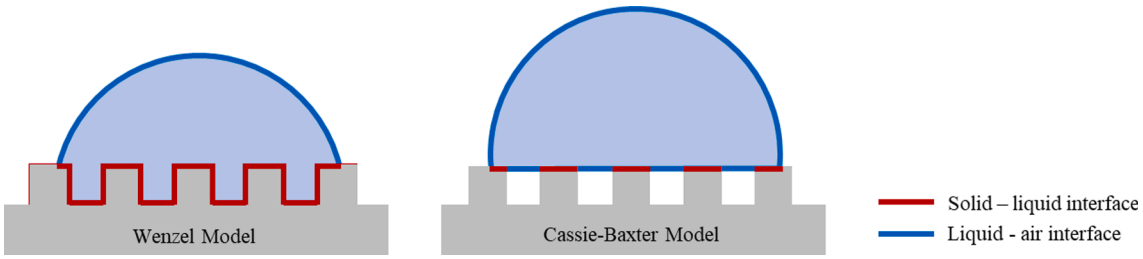

Fig. 5. Schematic representation of drop penetration into the asperities of the surface according to the Wenzel Model (left) and the Cassie-Baxter Model (right).

formation from condensed or incoming water when ice would normally form, i.e., at temperatures below water's freezing point, and/or weak shear and normal adhesion strength of ice (less than 100 kPa) (Hejazi et al., 2013). A parallel exists between the definitions of hydrophobicity and icephobicity, but hydrophobic and superhydrophobic surfaces are not always suitable for icephobic applications (Sojoudi et al., 2016).

Existing hydrophobic and hydrophilic nanotextures were tested by Jung et al. (Jung et al., 2011) and Eberle et al. (Eberle et al., 2014) to determine the characteristics of an ideal icephobic coating. A hydrophobic surface was observed to decrease the possibility of water freezing, while a hydrophilic surface delayed the freezing of supercooled droplets. As compared to the reference aluminum substrate, the ice nucleation was stopped at lower temperatures due to the presence of a hydration layer between the forming ice nucleus and the solid surface. However, the work (Schutzius et al., 2015a) on the physics of icing demonstrates that the surface nanoroughness influences nucleation delay but not nucleation temperature.

Frost formation can alter the wetting properties of a rough superhydrophobic surface, making it increasingly hydrophilic. The transition from the Cassie-Baxter to the Wenzel state takes place when the surface temperature decreases in a humid environment (Varanasi et al., 2010). This transition is verified when vapour condenses in the air pockets between the nanorough surface and the droplet and then begins freezing due to the low temperature. However, the self-cleaning capability of superhydrophobic surfaces may help prevent the Cassie-to-Wenzel transition (Sojoudi et al., 2016). Wang et al. (Wang et al., 2013) investigated droplet rebounds after hitting a surface: such events were found to be more probable on superhydrophobic surfaces with hierarchical structures than on micro- or nanostructured superhydrophobic surfaces. In fact, drop impact is a critical aspect for superhydrophobic surfaces, which do not implement nanotextured and closed-cell geometries, because the liquid meniscus may penetrate the surface texture (Schutzius et al., 2015b).

Snow deposits behave differently depending on snow characteristics: dry snow adhesion is regulated by solid–solid friction, while wet snow adhesion is regulated by solid–liquid friction. Therefore, dry snow sliding is accelerated on superhydrophobic surfaces, while wet snow slides off easily from hydrophilic surfaces. To prevent snow adhesion under both conditions, i.e., dry snow and wet snow, Nakajima et al. (Nakajima, 2004) developed a hybrid coating in which hydrophilic channels are realized on a superhydrophobic substrate.

Regarding the applications of these materials to PV, icephobic coatings should be selected by considering ice adhesion as a stress parameter. The design of icephobic surfaces presented in (Schutzius et al., 2015a) are characterized by ice-adhesion mean-stress values between 15 kPa and 60 kPa, while Golovin et al. (Golovin et al., 2016) designed coatings with ice adhesion values close to zero (0.2 kPa). There are some icephobic coatings that are available on the market, e.g., polysiloxanes, silicones, and anti-freezing proteins, and can be applied through rolling, brushing, or spraying on various substrates. Although their performance levels are generally worse than those of materials under development, e.g., laser-treated icephobic surfaces and silicone nanofilaments, they can achieve ice-adhesion mean-stress values ranging from 20 kPa to 80 kPa.

3. Materials and method

3.1. Workflow

The novelty of this study is in the development of a new workflow combining commonly used computational and analysis tools, e.g., PVSyst, with advanced algorithms from the literature, such as the MA (Marion et al., 2013). This research study is arranged into four stages (Fig. 6). The first to the third stages concern the solar assessment of different scenarios, i.e., the solar analysis of the PV system without the presence of snow, the solar analysis of the PV system considering snowfalls, and the solar analysis of the PV system enhanced with icephobic coatings and considering snowfalls. The fourth and final stage involves the estimation of the efficiency of the icephobic coatings and the comparison of the results.

During stage one, location, climate conditions, geometry, and ground albedo are considered as input values. The PVsyst tool, which implements the Perez sky diffuse model, is used to determine the POA irradiance of the PV system integrated into the building envelope case study. The typical meteorological year (TMY) weather data file, obtained through EnergyPlus weather (.epw), is used to describe climate conditions of Bergen, Oslo, and Trondheim (Norway). Conversely, the SD data are provided by the National Oceanic and Atmospheric Administration (NOAA) division in National Climatic Data Center (NCDC) in the US, as accessed via the national database of Norwegian Meteorological Institute using the eKlima service. A specific ground albedo value is assigned to each month, with the greater amounts corresponding to the winter season, when snow is deposited on the ground surface (Table 1).

During the second stage, the MA is integrated into the PVsyst calculation process to simulate the presence of snow deposits on PV panels and quantify the SL. Information about SD is considered as input, together with the parameters from the first stage, i.e., location, climate, geometry, and ground albedo. The functioning of the MA is detailed in this section.

In stage three, the investigated PV panels are enhanced with icephobic coatings. Therefore, the material's properties are considered as input parameters, in addition to those mentioned above. Similar to the method described for stage two, a co-simulation approach based on the combination of PVsyst and the MA is exploited.

Outputs from the three stages concern the POA irradiance amounts calculated for the three scenarios. Such quantities are post-processed in stage four to estimate the efficiency of the icephobic coatings, which is defined as the ratio between the SL estimated for PV panels enhanced with icephobic coatings and the SL estimated for traditional PV panels.

3.2. Case study locations and climates

The solar analyses are performed for the climate conditions characteristic of Bergen, Oslo, and Trondheim. According to the Köppen climate classification system, Bergen is classified as an oceanic climate (Cfb), Oslo as a warm-summer humid continental climate (Dfb), and Trondheim as a continental subarctic climate (Dfc), see Fig. 7.

Data about SD have been accessed through the Meteorological

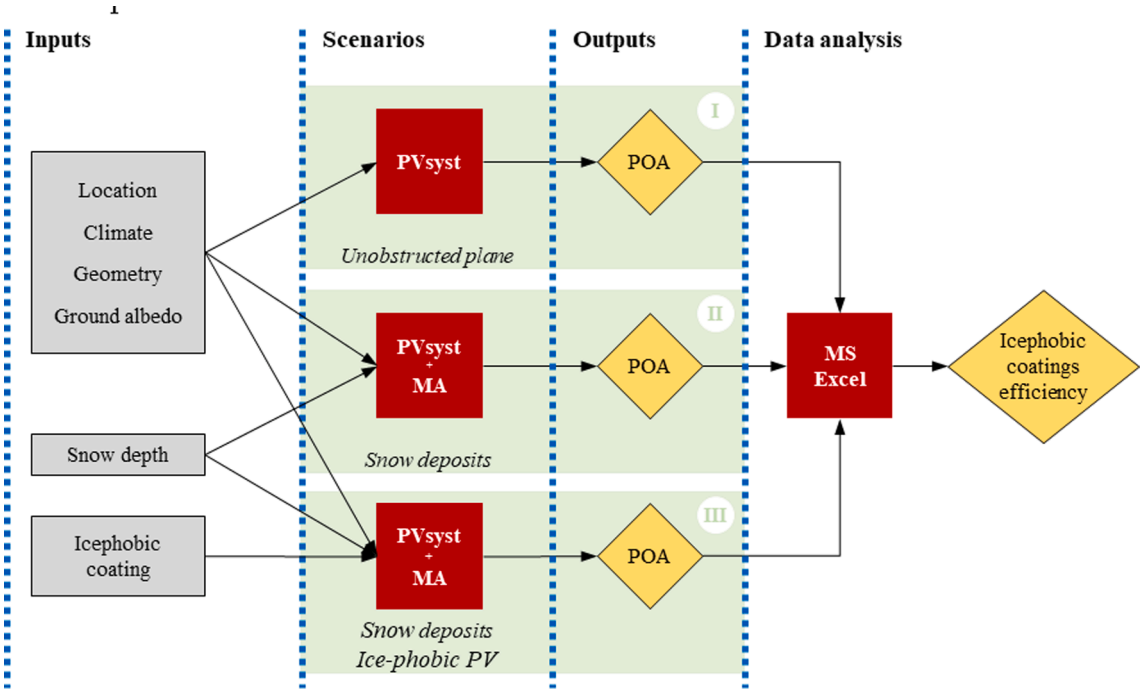

Fig. 6. The workflow of the conducted study: the boxes in grey are the input data; the red boxes represent the tools; in yellow, we present the output data; the green background identifies the three scenarios. (For interpretation of the references to colour in this figure legend, the reader is referred to the web version of this article.)

Table 1
Ground albedo values set in PVsyst for each month.

	Jan	Feb	Mar	Apr	May	Jun	Jul	Aug	Sep	Oct	Nov	Dec
Albedo	0.82	0.82	0.75	0.55	0.20	0.20	0.20	0.20	0.20	0.20	0.20	0.82

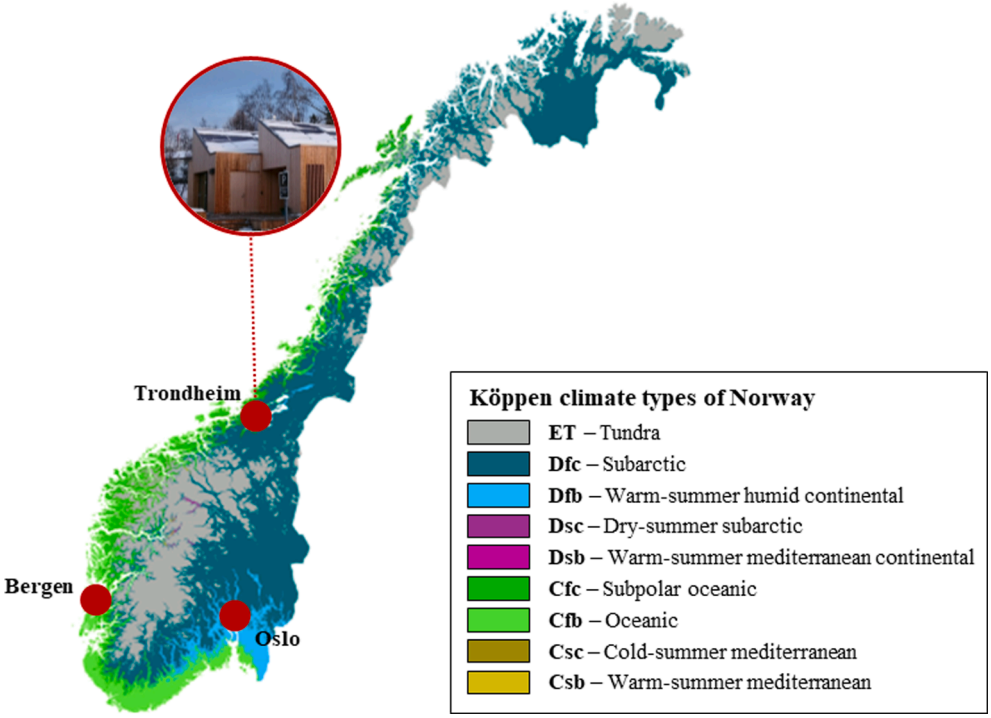

Fig. 7. The Köppen climate classification system: the case study locations and the building case study are reported in the circles. Modified from "Köppen climate types of Norway" by Adam Peterson.

Institute (MET). In Fig. 8, the monthly average SD values measured since January 2019 have been reported for Bergen, Oslo, and Trondheim. This time interval was chosen because it is the only one for which SD data are available for the three locations. Omitted months are characterized by null SD values.

3.3. Building case study: The ZEB Living Lab

The building case study is the ZEB Living Lab, in Trondheim. A detailed description of the facility and thee research activities performed there are provided in (Goia et al., 2015; Lobaccaro et al., 2017b).

The building is equipped with a PV system installed on the two south-facing roof slopes. The roof slopes have a tilt angle of 40° from the horizontal plane, and they are exposed southward. The PV system consists of 48 modules arranged in six rows of eight panels (three rows per roof slope). Each string is made of twelve PV panels (two strings per roof slope). The PV modules are REC 260PEs, and they have sixty polycrystalline silicon (poly-Si) solar cells, with three bypass diodes. The nominal power for one module is 260 W_p, for a total installed power of 11,480 W_p. The rated efficiency of the modules is 15.8%. The area of one module is 1.65 m^2 (1 m by 1.65 m), resulting in a total area of 79.2 m^2. Two Sunny Boy 5000 TL-21 MS inverters are installed (one per roof slope), which are characterized by a maximum DC power of 5.25 kW and an efficiency of around 97%.

In wintertime, the PV panels installed on the ZEB Living Lab are often subjected to snow cover, affecting energy production (Fig. 2) and exhibiting all the issues related to snow deposition for buildings at high latitudes. However, it is worth noting that this building presents a specific geometrical design for the roof, which is characterized by a tilted section 40° from the horizontal plane and a horizontal section. Even if this design represents a peculiar feature of a typical Norwegian dwelling on the one hand, the specific geometry of the building strongly influences the snow deposition on the other hand. In fact, the horizontal part of the roof represents a favorable place for snow accumulation, leading to a long period of snow coverage and ice formation, especially on the lowest PV rows during the coldest months. Consequently, the snow on the higher rows is prevented from sliding off. Even though this phenomenon was taken in consideration during the design phase by avoiding the installation of PV modules on the lowest part of the roof (Fig. 2), when abundant snow precipitation occurs, the PV modules are prevented from producing any energy because of the snow deposition and obstruction (Fig. 2). Further observations highlighted another problem that impedes snow sliding, the module frame; sometimes, the snow cover sticks to the frame and slides off only partially (Fig. 2).

3.4. Modelling snow losses

A new co-simulation method that combines the MA with commercial software, such as the PVsyst tool, is used to calculate SL. Firstly, the geometrical properties (i.e., tilt angle and azimuth angle) of the PV plant are defined, together with the location (i.e., latitude and longitude). Then, the POA irradiance is calculated by the PVsyst tool and then modified by the MA depending on the estimated snow coverage. The PVsyst software enables investigating grid-connected systems, stand-alone systems, pumping systems, and direct current networks for public transportation. The PVsyst tool also provides access to miscellaneous meteorological data sources, in addition to continuously updated solar system component data. These aspects make the PVsyst tool suitable for application to the wide range of studies that may follow the present one.

The PVsyst software allows us to account for "array incidence losses," which correspond to the decrease in the irradiance reaching the PV cell's surface due to reflections and the transmission of the sun's rays at each material interface, as well as to slight absorption of the glass cover. The magnitude of such an incidence effect increases with low incidence angle values for solar radiation; therefore, this issue should be particularly considered in Norway, especially during the winter. The PVsyst software program uses an incidence angle modifier (IAM) function based on the Fresnel's law, which describes the decrease in transmitted irradiance as a function of the incidence angle. This function is also applied to the beam component, as well as to the diffuse and albedo components.

The POA irradiance after the evaluation of the IAM losses is used by the MA to derive the snow coverage. In particular, the MA verifies the presence of snowfall events for each day. If a snowfall occurred, the model assumes that POA irradiance is null; otherwise, the latest snow coverage value from the day before is considered. This value is kept constant until either the POA irradiance or the air temperature changes, causing some of the accumulated snow to slide off. In fact, snow sliding occurs as long as the following inequality is satisfied:

$$T_a - \frac{POA}{m} > 0 \tag{2}$$

where T_a represents the hourly temperature of the air, expressed in Kelvin, and m represents Marion's empirically defined value (-80 W/m^2K).

If the model determines that sliding is possible, then the hourly snow slide amount is calculated according to the following:

$$s = k \cdot sin\beta \tag{3}$$

where the dimensionless sliding coefficient k is set equal to 1.97, which was experimentally determined for roof-mounted systems by Marion et al. (Marion et al., 2013), and β is the tilt angle in degrees. Once the snow slide amount is calculated, it is subtracted from the initial snow coverage until the volume of snow covering the PV modules is null. Finally, the PV strings that are free from snow are identified, and these PV modules are allowed to operate normally. Conversely, the energy production of the other PV strings is considered to be null. Such a routine is then reiterated for the following hour of the day.

3.5. Icephobic coatings

The behavior of icephobic coatings and their influences on snow adhesion to PV modules is simulated by modifying the sliding coefficient

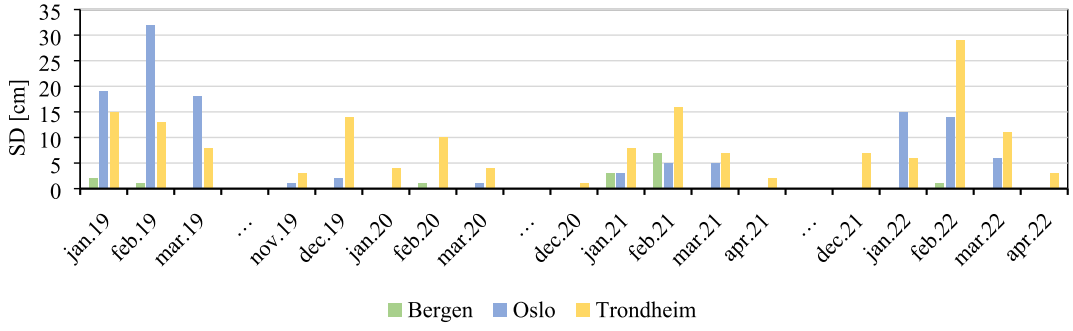

Fig. 8. Monthly average snow depth (SD) amounts calculated since January 2019 are reported for Bergen, Oslo, and Trondheim (Norway).

derived from the MA. Moving from the definition of the friction coefficient as the ratio between the shear force per unit area (S) and the pressure due to the load (P), the S-term can be defined as follows:

$$\frac{S}{P} = \frac{\sin\beta}{cos\beta} \tag{4}$$

When the icephobic coating is applied to the photovoltaic surface, the S value can change proportionally to the ratio between the ice adhesion strength of the panel surface treated with the icephobic coating and the ice adhesion strength of the untreated panel surface. Consequently, an equivalent sliding coefficient is defined bt dividing the value defined by Marion et al. (Marion et al., 2013) by the same ratio.

Icephobic coatings that are already on the market have been studied so as to allow for the full comprehension of their characteristics. Data sheets usually refer to an ice adhesion parameter to show the efficiency of the product. For the icephobic coatings available on the market, ice adhesion usually ranges between 40 kPa and 80 kPa.[1] Tests made on bare glass, which is the material commonly applied as a cover for PV panels, showed that ice adhesion can be assumed to be around 400 kPa (Chernyy et al., 2014). Therefore, comparing a value of around 60 kPa (i.e., in the middle of the above range) with the above given value of 400 kPa, the ice adhesion strength of PV panels enhanced with icephobic coatings may be assumed to be reduced by 85%; thus, the equivalent sliding coefficient is obtained by dividing the sliding coefficient for the untreated PV panel by 0.15.

3.6. Limitations and assumptions of the current study

The main limitations of this study are presented and discussed in the following. The data on solar irradiation from statistic-based weather data files may contain an incorrect computing of direct fractions, as well as systematic errors within the evaluation of the potential benefits. Such weather data files are, however, the usual source of weather data at the preliminary phase of the design process and are, at the moment, the most used and most accepted source of weather data inputs in terms of building performance simulations.

Concerning the PV applications of icephobic coatings, high transparency is required. Nonetheless, icephobic coatings are mostly opaque because the light transmittance usually decreases with increasing surface roughness. New technological solutions (Wu et al., 2022; Zhuo et al., 2020) have achieved high transparency and anti-reflective levels, but they may alter the optical properties of the PV panels. Therefore, modelling the icephobic coatings through only the MA's slide coefficient limits the results' overall accuracy. However, the workflow followed in this study is based on a comparative analysis of the results, and this significantly reduces the impact of this limitation on the main research outcomes.

The equivalent sliding coefficient (see Section 3.5) is not experimentally determined for the investigated icephobic coatings. However, the proposed workflow is developed to be exploited at the early stages of the design process, when material and technology solutions are still undefined. At these stages, architects, engineers, and designers can mostly rely on information reported on materials' data sheets. Therefore, the sliding coefficient is calculated from the ice adhesion parameter, which is usually provided in such documentation. Here as well, the comparative approach helps reduce the impact of this limitation.

The co-simulation approach, as described in this work, has not been validated against experimental data. Nonetheless, the accuracy of the two tools combined in this co-simulation approach, i.e., PVsyst and the MA, has already been widely addressed by other available studies in the literature (Nicolás-Martín et al., 2020; Øgaard et al., 2021).

Finally, the PV panels considered in this study are integrated on a tilted planar roof, which does not present any obstacles to snow sliding, e.g., windows, antennas, and chimneys. Similarly, the adhesion of snow to the frame of the PV modules is neglected when evaluating snow sliding.

4. Results and discussion

4.1. Scenario of snow losses in Norway without the application of icephobic photovoltaic surfaces

The average monthly amounts of POA irradiance for an unobstructed plane and SD are calculated over the monitored period (from 2019 to 2022) for the three case study locations (Fig. 9). Such POA irradiance values are used as references to determine the SL later. Only the months with SD amounts different from zero in at least one of the locations are included in the following analyses. This allows us to focus exclusively on those months in which icephobic coatings are effective so as to better understand the implications of their application. Therefore, only the months between November and April will be considered in the time domain from here on.

The results regarding the reduction of POA irradiance due to snow deposits (the scenario with the presence of snow) are reported in Fig. 10 and Table 2 for Oslo, Bergen, and Trondheim. Oslo shows the greatest variations from the reference irradiance profile in January (from 14.40 kWh/m^2 to 4.15 kWh/m^2), while the global solar irradiance impinging on the PV panels is halved in December. In Bergen, the SL were lower than in the other locations due to the warmer climate conditions. However, the POA irradiance was decreased by 20% in January and 15% in February (i.e., no significant variations detected during the other months). In Trondheim, SL are observed between December and March, with a peak in February (from 38.00 kWh/m^2 to 26.65 kWh/m^2). The total amounts of SL estimated for the selected months has confirmed Oslo as the case study with the highest snow loss percentage (around 15%), followed by Trondheim (around 10%) and Bergen (lower than 5%). It is worth highlighting that the PV panels in Bergen are also characterized by the lowest solar accessibility; therefore, the minimum potential for the application of icephobic coatings is observed for this case study. In fact, an ideal icephobic coating (i.e., a coating enabling a completely null SL) would allow harvesting only 5.85 kWh/m^2 in Bergen, as compared to 25.05 kWh/m^2 in Trondheim and 32.75 kWh/m^2 in Oslo.

4.2. Scenario with the application of icephobic photovoltaic surfaces

The reduction of POA irradiance due to snow deposits when icephobic coatings are applied to the PV panels' surfaces can be seen in Fig. 11 and Table 3 for Oslo, Bergen, and Trondheim. The SL percentages calculated for the PV plant in Oslo range between 40% and 50% of the POA irradiation estimated for an unobstructed surface, that is, during December and January. Conversely, minor losses, i.e., lower than 5%, are observed in the other months. In Bergen, the POA irradiance amount that is lost because of snow deposits is always lower than 2.00 kWh/m^2 per month, and the maximum loss is observed in February, at 1.50 kWh/m^2. Indeed, the trend of the POA irradiance estimated considering SL and solar panels enhanced with icephobic coatings does not diverge significantly from the reference POA irradiance (Fig. 11b). When icephobic coatings are applied to the solar panels in Trondheim, snow deposits prevent a share of the solar irradiance from being harvested, with a peak in February (around 20%). Icephobic coatings do not alter the rankings described in the previous section: Oslo is the case study location showing the highest SL (5%) throughout the considered months, followed by Trondheim (3%) and Bergen (2%). Despite the application of icephobic coatings, SL still account for 12.05 kWh/m^2 in Oslo, 3.35 kWh/m^2 in Bergen, and 10.00 kWh/m^2 in Trondheim throughout the considered months.

[1] https://www.silicone-polymers.co.uk/.

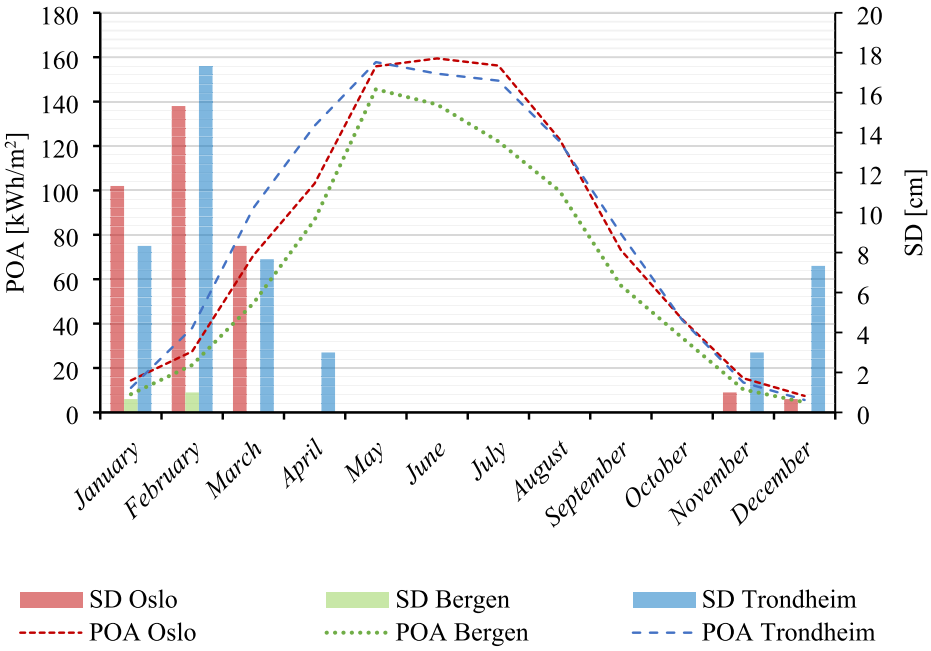

Fig. 9. The average monthly amounts of plane of array (POA) irradiance and snow depth (SD). The average is calculated over the monitored period (from 2019 to 2022) for the three case study locations.

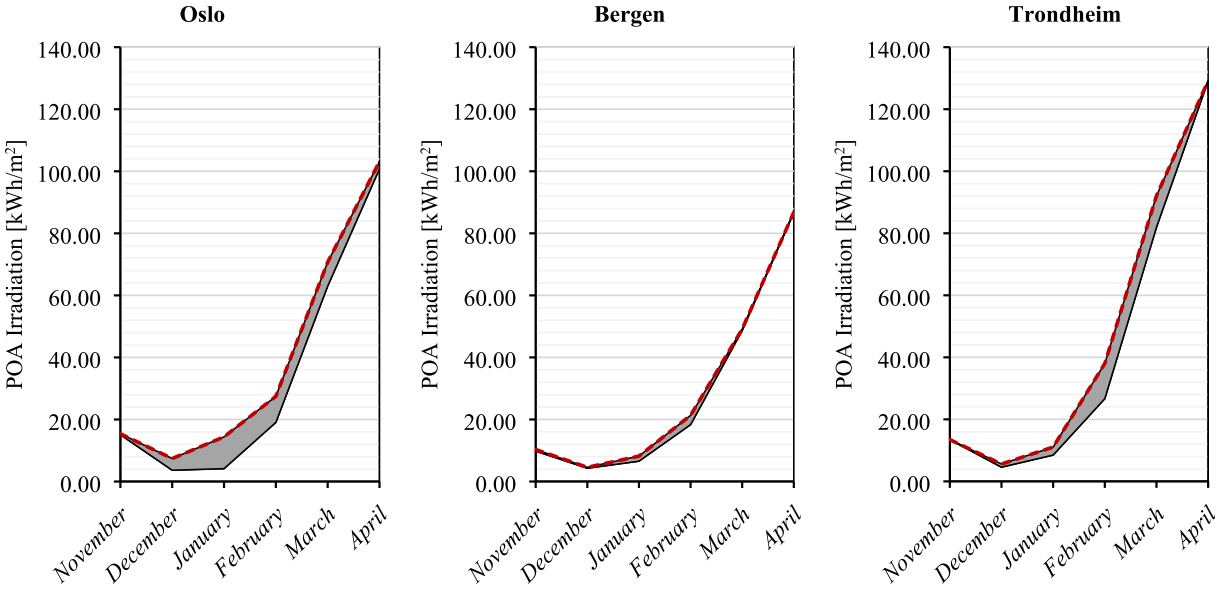

Fig. 10. Outcomes concerning the reduction of plane of array (POA) irradiation due to snow deposits (the scenario with the presence of snow) for Oslo, Bergen, and Trondheim (Norway). The dashed line and the gray area depict, respectively, the POA reference value and the solar energy loss due to snow from this when the presence of snow is considered.

Table 2
Outcomes of the solar analysis performed for the scenario with the presence of snow, considering the climates in Oslo, Bergen, and Trondheim (Norway).

	Oslo			Bergen			Trondheim		
	POA Irradiation [kWh/m²]	SL [kWh/m²]	SL [%]	POA Irradiation [kWh/m²]	SL [kWh/m²]	SL [%]	POA Irradiation [kWh/m²]	SL [kWh/m²]	SL [%]
November	15.40	0.30	2	10.30	0.50	5	13.50	0.00	0
December	7.40	3.80	51	4.60	0.30	6	5.60	1.00	18
January	14.40	10.25	71	8.20	1.65	20	11.05	2.60	23
February	27.45	8.40	31	21.30	3.00	14	38.00	11.35	30
March	70.70	7.75	11	49.15	0.50	1	92.05	10.15	11
April	103.10	2.30	2	86.80	0.00	0	129.15	0.00	0

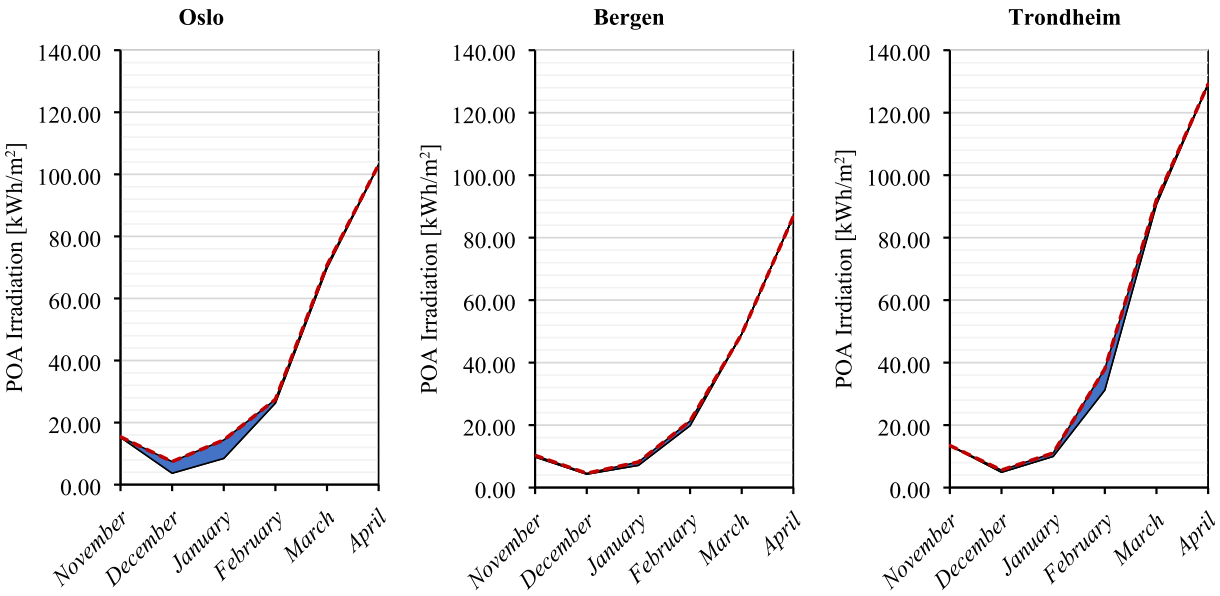

Fig. 11. Outcomes concerning reduction of plane of array (POA) irradiation due to snow deposits (scenario with the presence of snow and icephobic coatings applied to PV panels) in Oslo, Bergen, and Trondheim (Norway). The dashed line and the blue area depict, respectively, the POA reference value and the and the solar energy loss due to snow when snow presence and icephobic coatings are considered. (For interpretation of the references to colour in this figure legend, the reader is referred to the web version of this article.)

Table 3
Outcomes of a solar analysis performed for the scenario with the presence of snow and icephobic coatings applied to PV panels, considering the climates in Oslo, Bergen, and Trondheim (Norway).

	Oslo			Bergen			Trondheim		
	POA Irradiation [kWh/m²]	SL [kWh/m²]	SL [%]	POA Irradiation [kWh/m²]	SL [kWh/m²]	SL [%]	POA Irradiation [kWh/m²]	SL [kWh/m²]	SL [%]
November	15.40	0.15	1	10.30	0.50	5	13.45	0.00	0
December	7.40	3.75	50	4.55	0.25	6	5.60	0.70	12
January	14.40	5.95	41	8.20	1.05	13	11.05	1.10	10
February	27.45	1.15	4	21.30	1.50	7	38.00	6.80	18
March	70.70	0.90	1	49.15	0.00	0	92.05	1.45	2
April	103.10	0.15	0	86.80	0.00	0	129.15	0.00	0

4.3. Inter-scenario comparison and guidelines

The icephobic coatings simulated in this study were capable of reducing the SL in all the considered locations (Fig. 12). In Oslo, the solar irradiance harvested by the treated solar panels diverges from the reference value (i.e., the POA irradiance of an unobstructed plane) by 12.05 kWh/m^2, while the solar irradiance harvested by the untreated solar panels diverges by 32.75 kWh/m^2 throughout the selected months. According to this, the icephobic coatings are effective in reducing SL by around 65% during the winter. In Bergen, the application of icephobic coatings reduces SL from 5.85 kWh/m^2 to 3.35 kWh/m^2 between November and April, with an effectiveness of around 45%. In Trondheim, during the considered months, only 10.00 kWh/m^2 would not be harvested due to snow deposits if the solar panels were treated with icephobic coatings. Conversely, in the scenario without the application of icephobic photovoltaics, the SL amount to 25.05 kWh/m^2. The icephobic coatings are characterized by an effectiveness of 60% in the case study location of Trondheim. Exploiting icephobic coatings is more efficient in Oslo (65% efficiency) and in Trondheim (60% efficiency) than in Bergen (45% efficiency).

It is worth highlighting that the icephobic coatings are found to be more effective during the months between January and April than in November and December at every location (Fig. 12). Both the greater SD and the higher solar accessibility of the PV panels observed in the period from January to April contribute to increasing the icephobic coatings' efficiency. Furthermore, the best monthly effectiveness is found in March for Bergen when SL are lowered to zero, while the highest nominal reduction of SL is estimated in March for Trondheim (8.70 kWh/m^2).

To summarize, the following guidelines are outlined concerning the application of icephobic coatings in Norway:

- The application of icephobic coatings should be prioritized in locations classified as having a continental climate (zone D);
- Icephobic coatings should be applied to maximize PV power output between January and April in Oslo, as well as between January and March in Bergen and Trondheim;
- Icephobic coatings currently available on the market can reduce SL in solar panels by at least 45% during winter.

5. Conclusions and future outlook

This study presents an insight into the snow-related issues of photovoltaic (PV) plants at high latitudes. The proposed workflow moves from an assessment of snow deposits on PV panels and the consequent reduction of plane of array (POA) irradiance to an evaluation of the influence of icephobic nanomaterials on snow losses. These analyses are performed for three case study locations in Norway (Oslo, Bergen, and Trondheim).

When snow presence is considered, the SL calculated over the

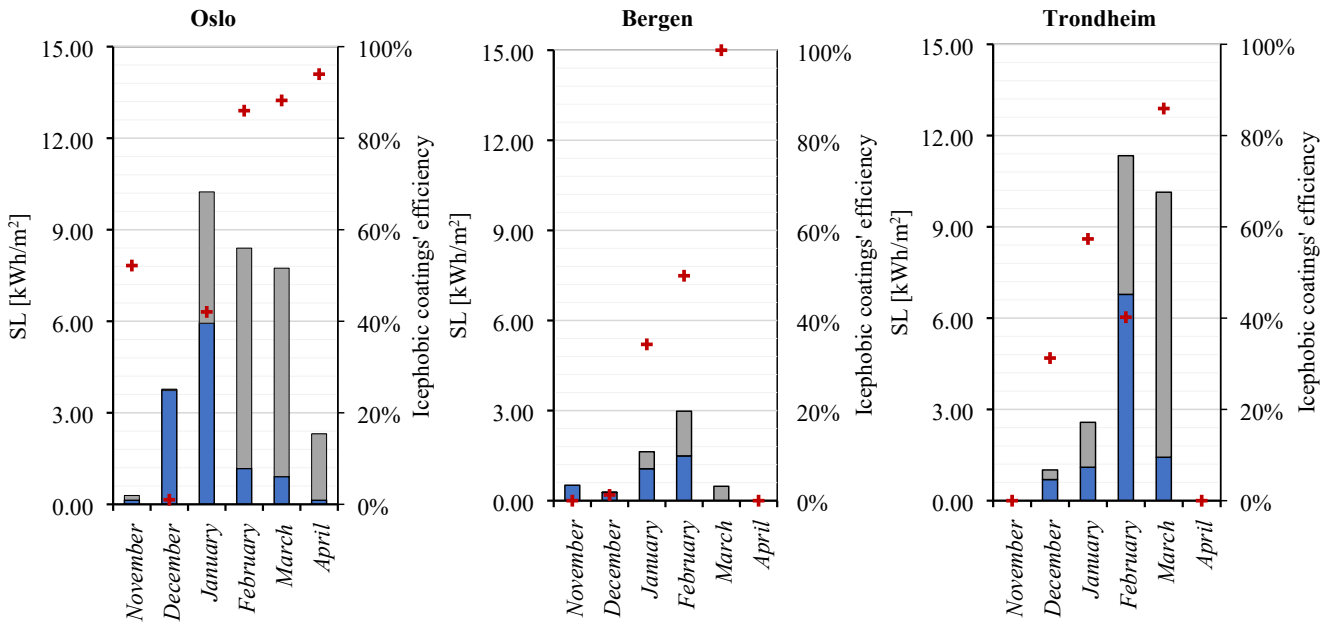

Fig. 12. SL and icephobic coatings' efficiency: the blue bars represent the SL when icephobic coatings are applied to PV panels; the grey bars describe the additional SL in the scenario without icephobic coatings, with the red cross symbols representing the icephobic coatings' efficiency. The efficiency of the icephobic coatings is defined as the ratio between the SL estimated for PV panels enhanced with icephobic coatings and the SL estimated for traditional PV panels. (For interpretation of the references to colour in this figure legend, the reader is referred to the web version of this article.)

months between November and April are equal to 32.75 kWh/m^2 in Oslo, 25.05 kWh/m^2 in Trondheim, and 5.85 kWh/m^2 in Bergen. In particular, the SL can amount to 70% of the POA irradiance (during January in Oslo). Therefore, techniques for snow removal should be implemented to boost solar energy penetration at high latitudes. The application of icephobic coatings currently available on the market can reduce SL to 12.05 kWh/m^2 in Oslo, 10.00 kWh/m^2 in Trondheim, and 3.35 kWh/m^2 in Bergen. Therefore, the effectiveness of the icephobic coatings is equal to 65% in Oslo, 60% in Trondheim, and 45% in Bergen.

If we consider an annual basis analysis, the SL account for a maximum of 3% of the yearly POA. Such a value is in line with that estimated by Becker et al. for Continental Europe (Becker et al., 2008). Therefore, the application of icephobic coatings cannot enable additional solar energy gains that exceed such a share of POA. This makes it necessary to accurately investigate the economic feasibility of the proposed technology regarding its application at high latitudes.

The main findings can be summarized as followings:

- Snow losses are larger in Oslo than in Trondheim and Bergen.
- The mitigation of SL due to icephobic coatings application is directly proportional to SL.
- The highest nominal reduction of SL is estimated for March in Trondheim (8.70 kWh/m^2).
- The highest monthly effectiveness is found for March in Bergen, when SL are nulled.

In conclusion, the application of icephobic coatings should be boosted at locations classified as having a continental climate (zone D in the Köppen climate classification system) to maximize PV power output during the wintertime on the one hand, as well as to enhance the performance level of other solar strategies, such as solar air heaters, light shelves, and photoluminescent surfaces, on the other hand. Nonetheless, for future studies, it will be important to gain further insight into the model chain, as well as the applied icephobic nanomaterials. This includes the following aspects:

- Validating the model chain with experimental data from various high-latitude locations and PV systems.
- Implementing a more accurate model chain for the better simulation of the behavior of icephobic coatings when applied to PV panels, i.e., modelling icephobic coatings otherwise than using Marion's algorithm (MA) for the sliding coefficient.
- Assessing the potential of icephobic coatings that have been presented in the literature but are not yet available in the commercial market.
- Conducting an economic analysis of the application of icephobic nanomaterials to PV panels, with a specific focus on the payback period of the intervention.
- Obtaining miscellaneous information about icephobic materials and coatings through the available literature and by conducting new laboratory experiments, e.g., transparency and anti-reflective levels, climate exposure and ageing durability, and snow/ice repulsion efficiency.
- Performing a sensitivity analysis of the ice adhesion strength of the PV panels.

Declaration of Competing Interest

The authors declare that they have no known competing financial interests or personal relationships that could have appeared to influence the work reported in this paper.

Acknowledgements

The authors acknowledge the Research Council of Norway to support this study within the research projects "Enhancing Optimal Exploitation of Solar Energy in Nordic Cities through the Digitalization of the Built Environment" (Helios, project no. 324243) and "Building Integrated Photovoltaics for Norway" (BIPV Norway, project no. 244031).

References

Andenæs, E., Jelle, B.P., Ramlo, K., Kolås, T., Selj, J., Foss, S.E., 2018. The influence of snow and ice coverage on the energy generation from photovoltaic solar cells. Sol. Energy 159, 318–328. https://doi.org/10.1016/J.SOLENER.2017.10.078.

Andersson, P.O., Jelle, B.P., Zhang, Z., 2017. Passive Snow Repulsion: A State-of-the-art Review Illuminating Research Gaps and Possibilities. Energy Procedia 132, 423–428. https://doi.org/10.1016/J.EGYPRO.2017.09.650.

Andrews, R.W., Pollard, A., Pearce, J.M., 2013a. The effects of snowfall on solar photovoltaic performance. Sol. Energy 92, 84–97. https://doi.org/10.1016/J.SOLENER.2013.02.014.

Andrews, R.W., Pollard, A., Pearce, J.M., 2013b. A new method to determine the effects of hydrodynamic surface coatings on the snow shedding effectiveness of solar photovoltaic modules. Sol. Energy Mater. Sol. Cells 113, 71–78. https://doi.org/10.1016/J.SOLMAT.2013.01.032.

Becker, G., Schiebelsberger, B., Weber, W., Schumacher, J., Zehner, M., Wotruba, G., Vodermayer, C., 2008. Energy yields of photovoltaic systems - Comparison of simulation and reality. https://doi.org/10.4229/23rdEUPVSEC2008-4BV.1.57.

Borrebæk, P.O.A., Jelle, B.P., Zhang, Z., 2020. Avoiding snow and ice accretion on building integrated photovoltaics – challenges, strategies, and opportunities. Sol. Energy Mater. Sol. Cells 206, 110306. https://doi.org/10.1016/J.SOLMAT.2019.110306.

Borrebæk, P.-O.-A., Rønneberg, S., Jelle, B.P., Klein-Paste, A., Zhang, Z., He, J., 2021. A framework for classification of snow- and icephobicity. J. Adhes. Sci. Technol. 35, 1087–1098. https://doi.org/10.1080/01694243.2020.1834286.

Chernyy, S., Järn, M., Shimizu, K., Swerin, A., Pedersen, S.U., Daasbjerg, K., Makkonen, L., Claesson, P., Iruthayaraj, J., 2014. Superhydrophilic polyelectrolyte brush layers with imparted anti-icing properties: effect of counter ions. ACS Appl. Mater. Interfaces 6, 6487–6496. https://doi.org/10.1021/am500046d.

Dubey, S., Sarvaiya, J.N., Seshadri, B., 2013. Temperature dependent photovoltaic (PV) efficiency and its effect on PV production in the world - A review, in: Energy Procedia. Elsevier, pp. 311–321. https://doi.org/10.1016/j.egypro.2013.05.072.

Eberle, P., Tiwari, M.K., Maitra, T., Poulikakos, D., 2014. Rational nanostructuring of surfaces for extraordinary icephobicity. Nanoscale 6, 4874–4881. https://doi.org/10.1039/C3NR06644D.

Fillion, R.M., Riahi, A.R., Edrisy, A., 2014. A review of icing prevention in photovoltaic devices by surface engineering. Renew. Sustain. Energy Rev. 32, 797–809. https://doi.org/10.1016/J.RSER.2014.01.015.

Formolli, M., Lobaccaro, G., Kanters, J., 2021. Solar energy in the Nordic built environment: challenges, opportunities and barriers. Energies 14. https://doi.org/10.3390/en14248410.

Goia, F., Finochiaro, L., Gustavsen, A., 2015. The ZEB Living Laboratory at the Norwegian University of Science and Technology: a zero emission house for engineering and social science experiments.

Golovin, K., Kobaku, S.P.R., Lee, D.H., DiLoreto, E.T., Mabry, J.M., Tuteja, A., 2016. Designing durable icephobic surfaces. Sci. Adv. 2, e1501496.

Good, C.S., Lobaccaro, G., Hårklau, S., 2014. Optimization of solar energy potential for buildings in urban areas - A Norwegian case study, in: Energy Procedia. Elsevier, pp. 166–171. https://doi.org/10.1016/j.egypro.2014.10.424.

Hejazi, V., Sobolev, K., Nosonovsky, M., 2013. From superhydrophobicity to icephobicity: forces and interaction analysis. Sci. Rep. 3, 2194. https://doi.org/10.1038/srep02194.

Jelle, B.P., 2013. The challenge of removing snow downfall on photovoltaic solar cell roofs in order to maximize solar energy efficiency—Research opportunities for the future. Energy Build. 67, 334–351. https://doi.org/10.1016/J.ENBUILD.2013.08.010.

Jelle, B.P., 2016. Building Integrated Photovoltaics: A Concise Description of the Current State of the Art and Possible Research Pathways. Energies 9. https://doi.org/10.3390/en9010021.

Jelle, B.P., Breivik, C., Drolsum Røkenes, H., 2012. Building integrated photovoltaic products: A state-of-the-art review and future research opportunities. Sol. Energy Mater. Sol. Cells 100, 69–96. https://doi.org/10.1016/J.SOLMAT.2011.12.016.

Jelle, B.P., Gao, T., Mofid, S.A., Kolås, T., Stenstad, P.M., Ng, S., 2016. Avoiding Snow and Ice Formation on Exterior Solar Cell Surfaces – A Review of Research Pathways and Opportunities. Procedia Eng. 145, 699–706. https://doi.org/10.1016/J.PROENG.2016.04.084.

Jouttijärvi, S., Lobaccaro, G., Kamppinen, A., Miettunen, K., 2022. Benefits of bifacial solar cells combined with low voltage power grids at high latitudes. Renew. Sustain. Energy Rev. 161, 112354 https://doi.org/10.1016/J.RSER.2022.112354.

Jung, S., Dorrestijn, M., Raps, D., Das, A., Megaridis, C.M., Poulikakos, D., 2011. Are superhydrophobic surfaces best for icephobicity? Langmuir 27, 3059–3066. https://doi.org/10.1021/la104762g.

Lobaccaro, G., Carlucci, S., Croce, S., Paparella, R., Finocchiaro, L., 2017a. Boosting solar accessibility and potential of urban districts in the Nordic climate: A case study in Trondheim. Sol. Energy 149, 347–369. https://doi.org/10.1016/J.SOLENER.2017.04.015.

Lobaccaro, G., Esposito, S., Goia, F., Perino, M., 2017b. Daylighting availability in a living laboratory single family house and implication on electric lighting energy demand. Energy Procedia 122, 601–606. https://doi.org/10.1016/j.egypro.2017.07.356.

Manni, M., Lobaccaro, G., Goia, F., Nicolini, A., 2018. An inverse approach to identify selective angular properties of retro-reflective materials for urban heat island mitigation. Sol. Energy 176, 194–210. https://doi.org/10.1016/J.SOLENER.2018.10.003.

Manni, M., Lobaccaro, G., Lolli, N., Bohne, R.A., 2020. Parametric Design to Maximize Solar Irradiation and Minimize the Embodied GHG Emissions for a ZEB in Nordic and Mediterranean Climate Zones. Energies 13. https://doi.org/10.3390/en13184981.

Marion, B., Schaefer, R., Caine, H., Sanchez, G., 2013. Measured and modeled photovoltaic system energy losses from snow for Colorado and Wisconsin locations. Sol. Energy 97, 112–121. https://doi.org/10.1016/J.SOLENER.2013.07.029.

Midtdal, K., Jelle, B.P., 2013. Self-cleaning glazing products: A state-of-the-art review and future research pathways. Sol. Energy Mater. Sol. Cells 109, 126–141. https://doi.org/10.1016/J.SOLMAT.2012.09.034.

Nakajima, A., 2004. Design of a transparent hydrophobic coating. J. Ceram. Soc. Japan 112, 533–540. https://doi.org/10.2109/jcersj.112.533.

Nicolás-Martín, C., Eleftheriadis, P., Santos-Martín, D., 2020. Validation and self-shading enhancement for SoL: A photovoltaic estimation model. Sol. Energy 202, 386–408. https://doi.org/10.1016/J.SOLENER.2020.03.099.

Nocente, A., Time, B., Mathisen, H.M., Kvande, T., Gustavsen, A., 2021. The ZEB Laboratory: the development of a research tool for future climate adapted zero emission buildings. J. Phys. Conf. Ser. 2069, 12109. https://doi.org/10.1088/1742-6596/2069/1/012109.

Øgaard, M.B., Aarseth, B.L., Skomedal, Å.F., Riise, H.N., Sartori, S., Selj, J.H., 2021. Identifying snow in photovoltaic monitoring data for improved snow loss modeling and snow detection. Sol. Energy 223, 238–247. https://doi.org/10.1016/J.SOLENER.2021.05.023.

Parvate, S., Dixit, P., Chattopadhyay, S., 2020. Superhydrophobic surfaces: insights from theory and experiment. J. Phys. Chem. B 124, 1323–1360. https://doi.org/10.1021/acs.jpcb.9b08567.

Powers, L., Newmiller, J., Townsend, T., 2010. Measuring and modeling the effect of snow on photovoltaic system performance, in: 2010 35th IEEE Photovoltaic Specialists Conference. pp. 973–978. https://doi.org/10.1109/PVSC.2010.5614572.

Ross, M.M.D., 1995. Snow and ice accumulation on photovoltaic arrays: An assessment of the TN conseil passive melting technology. Varennes.

Scharmer Grief, J., K.,, 2000. The European solar radiation atlas. Les Presses de L'École des Mines, Paris.

Schutzius, T.M., Jung, S., Maitra, T., Eberle, P., Antonini, C., Stamatopoulos, C., Poulikakos, D., 2015a. Physics of icing and rational design of surfaces with extraordinary icephobicity. Langmuir 31, 4807–4821. https://doi.org/10.1021/la502586a.

Schutzius, T.M., Jung, S., Maitra, T., Graeber, G., Köhme, M., Poulikakos, D., 2015b. Spontaneous droplet trampolining on rigid superhydrophobic surfaces. Nature 527, 82–85. https://doi.org/10.1038/nature15738.

Şevik, S., Aktaş, A., 2022. Performance enhancing and improvement studies in a 600 kW solar photovoltaic (PV) power plant; manual and natural cleaning, rainwater harvesting and the snow load removal on the PV arrays. Renew. Energy 181, 490–503. https://doi.org/10.1016/J.RENENE.2021.09.064.

Sojoudi, H., Wang, M., Boscher, N.D., McKinley, G.H., Gleason, K.K., 2016. Durable and scalable icephobic surfaces: similarities and distinctions from superhydrophobic surfaces. Soft Matter 12, 1938–1963. https://doi.org/10.1039/C5SM02295A.

Statista, 2022. Solar energy capacity in Norway from 2010 to 2021 [WWW Document]. URL https://www.statista.com/statistics/1165971/total-solar-power-capacity-in-norway/.

Tina, G.M., Scavo, F.B., Aneli, S., Gagliano, A., 2021. Assessment of the electrical and thermal performances of building integrated bifacial photovoltaic modules. J. Clean. Prod. 313, 127906 https://doi.org/10.1016/J.JCLEPRO.2021.127906.

Varanasi, K.K., Deng, T., Smith, J.D., Hsu, M., Bhate, N., 2010. Frost formation and ice adhesion on superhydrophobic surfaces. Appl. Phys. Lett. 97, 234102 https://doi.org/10.1063/1.3524513.

Wang, Y., Xue, J., Wang, Q., Chen, Q., Ding, J., 2013. Verification of icephobic/anti-icing properties of a superhydrophobic surface. ACS Appl. Mater. Interfaces 5, 3370–3381. https://doi.org/10.1021/am400429q.

Wu, S., Liang, Z., Li, Y., Chay, S., He, Z., Tan, S., Wang, J., Zhu, X., He, X., 2022. Transparent, Photothermal, and Icephobic Surfaces via Layer-by-Layer Assembly. Adv. Sci. 9, 2105986. 10.1002/advs.202105986.

Xue, C.-H., Jia, S.-T., Zhang, J., Ma, J.-Z., 2010. Large-area fabrication of superhydrophobic surfaces for practical applications: an overview. Sci. Technol. Adv. Mater. 11, 33002. https://doi.org/10.1088/1468-6996/11/3/033002.

Zhuo, Y., Xiao, S., Håkonsen, V., Li, T., Wang, F., He, J., Zhang, Z., 2020. Ultrafast self-healing and highly transparent coating with mechanically durable icephobicity. Appl. Mater. Today 19, 100542. 10.1016/j.apmt.2019.100542.